analytical chemistry

Article

Cite This: Anal. Chem. 2018, 90, 5612−5619

pubs.acs.org/ac

Rapid In Situ Profiling of Lipid C═C Location Isomers in Tissue Using Ambient Mass Spectrometry with Photochemical Reactions

Fei Tang,[*,†,‡] Chengan Guo,[†,‡] Xiaoxiao Ma,[†] Jian Zhang,[†] Yuan Su,[§] Ran Tian,[§,∥] Riyi Shi,[§,∥] Yu Xia,[⊥,#] Xiaohao Wang,[†] and Zheng Ouyang[*,†,§]

[†]State Key Laboratory of Precision Measurement Technology and Instruments, Department of Precision Instrument, Tsinghua University, Beijing 100084, China

[§]Weldon School of Biomedical Engineering, Purdue University, West Lafayette, Indiana 47907, United States

[∥]Department of Basic Medical Sciences, College of Veterinary Medicine, Purdue University, West Lafayette, Indiana 47907, United States

[⊥]Department of Chemistry, Tsinghua University, Beijing 100084, China

[#]Department of Chemistry, Purdue University, West Lafayette, Indiana 47907, United States

Supporting Information

ABSTRACT: Rapid and in situ profiling of lipids using ambient mass spectrometry (AMS) techniques has great potential for clinical diagnosis, biological studies, and biomarker discovery. In this study, the online photochemical reaction involving carbon−carbon double bonds was coupled with a surface sampling technique to develop a direct tissue-analysis method with specificity to lipid C═C isomers. This method enabled the in situ analysis of lipids from the surface of various tissues or tissue sections, which allowed the structural characterization of lipid isomers within 2 min. Under optimized reaction conditions, we have established a method for the relative quantitation of lipid C═C location isomers by comparing the abundances of the diagnostic ions arising from each isomer, which has been proven effective through the established linear relationship (R^2 = 0.999) between molar ratio and diagnostic ion ratio of the FA 18:1 C═C location isomers. This method was then used for the rapid profiling of unsaturated lipid C═C isomers in the sections of rat brain, lung, liver, spleen, and kidney, as well as in normal and diseased rat tissues. Quantitative information on FA 18:1 and PC 16:0−18:1 C═C isomers was obtained, and significant differences were observed between different samples. To the best of our knowledge, this is the first study to report the direct analysis of lipid C═C isomers in tissues using AMS. Our results demonstrated that this method can serve as a rapid analytical approach for the profiling of unsaturated lipid C═C isomers in biological tissues and should contribute to functional lipidomics and clinical diagnosis.

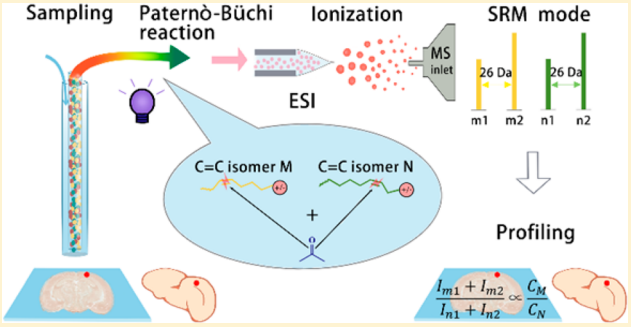

Lipids are hydrophobic or amphipathic small metabolites[1] that play a multitude of crucial roles in cells, tissues, and organ physiology, including energy storage, cell-to-cell signaling, and the formation of cell membranes.[2] The ability of an individual lipid (or class of lipids) to perform its biochemical and biophysical roles relies on its chemical structure. The alterations in lipid structures can lead to altered properties. As one of the most important parameters determining the overall shape of a lipid, the location of C═C bonds in unsaturated lipids is closely related to the biological function. For instance, omega-3 fatty acids (also called ω-3 fatty acids or n-3 fatty acids), polyunsaturated fatty acids (PUFAs) with the final double bond at the n-3 position, were found to be important in brain development and visual functions.[3,4] In addition, it is generally believed that omega-6 fatty acids are associated with chronic inflammatory effects, while omega-3 fatty acids have anti-inflammatory properties.[5] There have also been some studies investigating the effect of double-bond position on lipid bilayer properties. For instance, the study by Martinez-Seara et al. provided insight into the role of double bonds in lateral pressure profiles, lateral membrane dynamics, and intramolecular dynamics.[6,7] These studies highlighted the significance of double-bond position at the molecular level. Furthermore, extensive studies have demonstrated the consistent alternations of lipids and lipid C═C isomers compositions in diseased tissue.[8,9] For example, significant differences have been observed for concentration ratios of C═C location isomers from several fatty acid (FA) and glycerophospholipid (GP) species between normal and cancerous mouse breast tissues.[9] To facilitate rapid point-of-care

Received: November 13, 2017
Accepted: April 6, 2018
Published: April 6, 2018

DOI: 10.1021/acs.analchem.7b04675
Anal. Chem. 2018, 90, 5612−5619

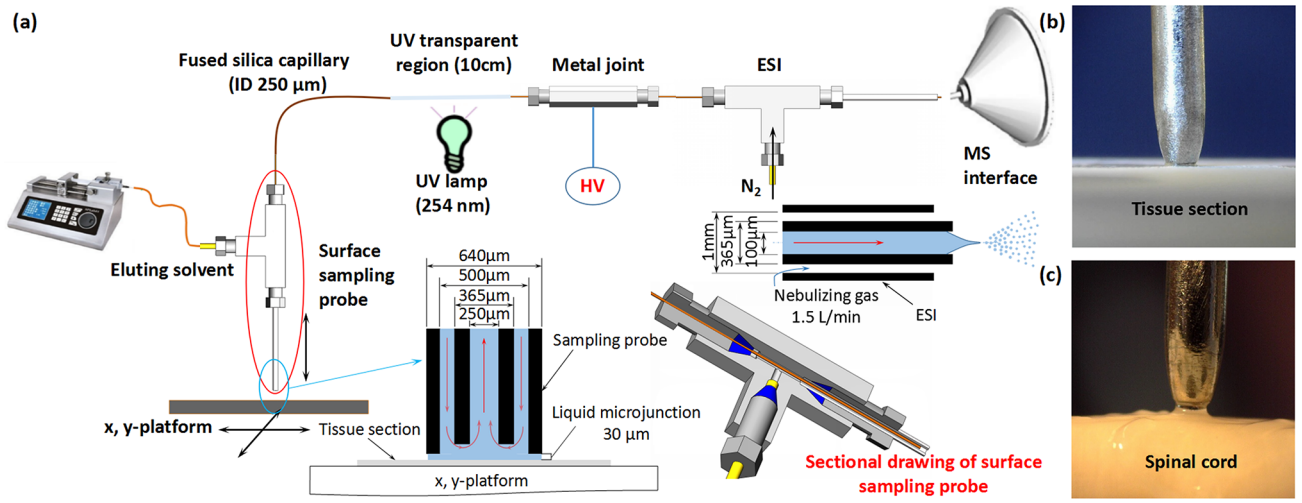

Figure 1. (a) Schematic of the experimental setup for profiling unsaturated lipid isomers. (b) Direct sampling of tissue section. (c) Direct sampling of mouse spinal cord.

(POC) diagnostics, it is therefore important to develop technologies with the power for rapid and in situ profiling of unsaturated lipid C=C location isomers.

Mass spectrometry (MS) is the most widely used analytical tool in the field of lipidomics, and a series of MS-based methods were developed to structurally characterize the positions of double bonds within a lipid molecule. Conventionally, MS in conjunction with chromatographic approaches, such as thin-layer chromatography (TLC),[10] gas chromatography (GC),[11,12] and liquid chromatography (LC),[13] were major tools for the analysis of lipids isomers in biological samples. However, the combination of chromatographic separation and MS is insufficient for structure elucidation. A reliable method for identification of the C=C location in lipids involves combining LC-MS with online derivatization following separation, for instance, in-line ozonolysis reaction[14] or ozone-induced dissociation (OzID).[15] However, LC-MS is both labor-intensive and time-consuming. Direct-infusion electrospray ionization (ESI) MS or matrix-assisted laser desorption/ionization mass spectrometry (MALDI MS) was developed to speed up lipid analysis without involving chromatographic separation. In this approach, MS^n or ozonolysis-induced dissociation was employed for the generation of diagnostic ions indicative of the C=C locations. Some notable methods include radical directed dissociation (RDD),[16] OzID,[17] low-energy multistage MS,[18] ozone electrospray ionization (OzESI),[19] electron-induced dissociation (EID),[20] helium metastable atom-activated dissociation (He-MAD),[21] electron impact excitation of ions from organics (EIEIO),[22] electron-capture dissociation (ETD),[23] ozonolysis-MALDI,[24] and MALDI-SpiralTOF (TOF = time-of-flight).[25] Each method has its own unique advantages, but special MS instruments are typically required, which has limited their widespread use. More importantly, direct-infusion ESI MS and MALDI MS still require multistep sample preparations. In contrast, in AMS, the ionization process is carried out outside the instrument in the laboratory environment or in samples' own natural environment, with no or minimal effort for sample preparation.[26,27] Because of the development of AMS techniques, sample preparation has been greatly simplified and the in situ analysis of lipid species in complex biological samples has been realized. To date, a number of AMS techniques have been used for direct lipid analysis,[28−39] and some studies have showcased the potential of AMS techniques in disease diagnosis, POC diagnostics, and therapeutic drug monitoring.[40−48] Recently, AMS techniques were also used for rapid identification of C=C isomers, such as low-temperature plasma (LTP),[49] desorption electrospray ionization−collision-induced dissociation/OzID (DESI-CID/OzID),[50] and ozonolysis-DESI.[51] These methods allow facile analysis of lipids isomers and are widely applied in both lipid identification and quantitation.

In this work, we report an AMS technique by coupling the online photochemical reaction (i.e., Paternò−Büchi reaction (PB reaction))[52] and tandem MS with in situ lipid extraction and ionization to develop a direct tissue-analysis method for the identification and quantitation of lipid C=C location isomers. A liquid microjunction surface sampling probe (LMJ-SSP)[53−58] was constructed to extract lipids from the tissue surface for MS analysis. Within 2 min, the C=C locations for lipids of interest were determined and relative quantitation of the lipid C=C location isomers was achieved. Using this method, we analyzed lipid C=C location isomer compositions in various kinds of rat tissue sections, including normal and diseased rat tissues. This method was demonstrated to be capable of the rapid profiling of lipid C=C location isomers in biological tissues and should contribute to MS imaging (MSI), functional lipidomics, and clinical diagnosis.

EXPERIMENTAL SECTION

Chemicals and Reagents. Oleic acid (FA 18:1 (9Z)), *cis*-vaccenic acid (FA 18:1 (11Z)), and 2-oleoyl-1-palmitoyl-*sn*-glycero-3-phosphocholine (PC 16:0/18:1 (9Z)) were purchased from Sigma-Aldrich (MO, U.S.A.). Methanol (MeOH), ethanol, and acetone of high-performance liquid chromatography (HPLC) grade were purchased from Merck (Darmstadt, Germany). Ultrapure water was obtained from a Millipore Milli-Q integral water-purification system (Bedford, MA, U.S.A.). Ammonium hydroxide (Macron Fine Chemicals; Center Valley, PA, U.S.A.) and formic acid (Mallinckrodt Chemicals; Hazelwood, MO, U.S.A.) were used as solution modifiers to enhance lipid ionization in the negative and positive ESI modes, respectively. All lipid standards were diluted to 10 μM in ethanol.

DOI: 10.1021/acs.analchem.7b04675
Anal. Chem. 2018, 90, 5612−5619

In Situ Lipid Extraction, Ionization, and MS Analysis. The detailed parameters of this homemade LMJ-SSP/PB reaction/ESI apparatus for unsaturated lipid C=C isomers profiling are shown in Figure 1. Two pieces (i.d. 250 μm/o.d. 365 μm and ~20 cm long, from surface sampling probe to metal joint; i.d. 150 μm/o.d. 365 μm and ~10 cm long, from metal joint to ESI) of fused silica capillary (Polymicro Technologies, Phoenix, AZ, U.S.A.) were used to deliver the solvent. The polyimide coating of a 10-cm-long fused silica capillary between the probe and metal joint was burnt off, forming a UV-transparent region (reaction zone). A low-pressure mercury lamp (model 80-1057-01, BHK, Inc., Ontario, CA, U.S.A.) was used to apply UV irradiation at 254 nm to facilitate the PB reaction between the unsaturated lipids and the acetone. The samples were fixed on a moving *x*,*y*-platform (MTS50-Z8, Thorlabs, Newton, NJ, U.S.A.), which was controlled by homemade software. The stage and probe were monitored using a digital USB Dino-Lite AM4515ZT Edge Microscope (AnMo Electronics Corporation), and the monitoring camera was focused on the liquid microjunction. The photo of this apparatus is shown in Figure S1.

Method Validation. For the method validation, test samples of standards were prepared. Polytetrafluoroethylene (PTFE)-printed slides (Cat. no. 63425-05, Electron Microscopy Sciences, Fort Washington, PA, U.S.A.) were used. The slides contained 12 5-mm wells surrounded by a hydrophobic PTFE coating, which restricted the solutions within the wells. The test samples were prepared by spotting a 10 μL FA 18:1 (11Z) solution and PC 16:0/18:1 (9Z) solution onto the well area of a PTFE-printed slide and allowing it to dry.

Sample Preparation for Relative Quantitation of Lipid C=C Isomers. To validate relative quantitation of lipid C=C location isomers, mixtures of two lipid C=C location isomers were prepared. Appropriate amounts of FA 18:1 (11Z) solution and FA 18:1 (9Z) solution were mixed to make mixture solutions with concentration ratios of 20:1, 10:1, 5:1, 2:1, 1:1, 1:2, 1:5, 1:10, and 1:20. The total concentration of FA 18:1 in all mixtures is still 10 μM. A mixture solution of 10 μL was added onto a well of the PTFE-printed slide and allowed to dry to make one sample. At each ratio, 5 on-surface samples were prepared.

Tissue Preparation and Sectioning. Animal care procedures were performed in accordance with the Purdue University Animal Care and Use Committee guidelines and ARRIVE guidelines. All tissue samples were provided by Harlan Laboratory (Indianapolis, IN, U.S.A.). The rat tissues, including brains, kidneys, lungs, livers, and spleens, were removed from the bodies of male Sprague–Dawley rats and immediately frozen at −80 °C. Tissue sections (30 μm) were obtained by a cryotome (Shandon Cryotome FE Thermo Scientific, Waltham, MA, U.S.A.) and mounted onto adhesive slides. Prior to analysis, the sections were dried in a desiccator for 1 h; then the sampling points that were uniformly distributed in the section were marked using red marker pen on the back of the slide, and optical images of the tissue sections were taken using a digital USB Dino-Lite AM4515ZT Edge microscope.

Disease Mouse Model Tissue Specimens. Disease samples, including cancerous mouse breast tissues and inflamed mouse spinal cord tissues, were collected from a rat breast cancer model and rat spinal cord contusion injury model, respectively, to use for clinical application tests. All samples were frozen at −80 °C. Before analysis, the sample was gradually thawed in a −20 °C freezer and then at 4 °C for 1 h, respectively.

Mass Spectrometry and Apparatus. All experiments were performed on a TSQ Quantum Access MAX (Thermo Scientific, San Jose, CA, U.S.A.) in the full-scan mode or selected reaction monitoring (SRM) mode. For the FA analysis, ESI was performed in the negative ion mode with a spray voltage at −3.6 kV; for the PC analysis, ESI was performed in the positive ion mode with a spray voltage at +5.5 kV. Other parameters of SRM mode, such as collision energy (CE) and the tube lens, are shown in Table 1.

Table 1. MS/MS Setting for SRM

compound	parent (*m*/*z*)	product (*m*/*z*)	tube lens (V)	CE (eV)
PC 16:0−18:1	818.5	650.5	116	19
	818.5	676.5	119	19
	818.5	678.5	119	19
	818.5	704.5	122	19
FA 18:1	339.3	171.1	102	25
	339.3	197.2	100	25
	339.3	199.2	100	25
	339.3	225.2	98	25

When using the LMJ-SSP/PB reaction/ESI apparatus, the eluting solvent was delivered by a syringe pump at 6 μL/min, and the aspiration rate of the probe was adjusted to match the pumped flow rate by adjusting the nebulizing gas flow rate (~1.5 L/min) to form a stable liquid microjunction (~30 μm thick). A 70/30 acetone/water (v/v) solution with 1% ammonium hydroxide was used to extract FA and a 60/20/20 acetone/methanol/water (v/v/v) solution with 1% formic acid was used to extract PC from the tissue or tissue section.

RESULTS AND DISCUSSION

Workflow for the LMJ-SSP/PB Reaction/ESI-MS Analysis. As shown in Figure 2, the tissue section to be analyzed was mounted on the *x*,*y*-platform. A syringe pump drove the eluting solvent (including acetone, one reactant of the PB reaction) to the sample surface, and the solvent was sprayed with nebulizing gas for ionization after the extraction. The whole process tooks only ~2 min as the solvent flow rate was set to 6 μL/min. Unsaturated lipids in the tissue were extracted by the solvent in contact with the tissue surface. The extracted unsaturated lipids were then allowed to react with acetone under UV irradiation for 50 s. PB products were then ionized and introduced into the mass spectrometer for MS and MS/MS analysis. PB reaction products had a mass increase of 58 Da compared to their lipid precursors. Low-energy collision-induced dissociation (CID) of PB reaction products produced abundant fragment ions specific to the C=C location (diagnostic ions). Meanwhile, the ion abundance of the diagnostic ions correlated with the relative amounts of lipid C=C location isomers, which could be used for the relative and even absolute quantitation of lipid C=C location isomers.[9]

Taking FA 18:1 (9Z) and FA 18:1 (11Z) as an example, these two fatty acid C=C isomers reacted with acetone under UV irradiation at 254 nm, forming four PB products at *m*/*z* 339. These PB products were ionized simultaneously by ESI and mass-isolated for subsequent CID. One pair of C=C diagnostic ions was produced for the 9Z or 11Z FA isomer, i.e., *m*/*z* 171 and *m*/*z* 197 for FA 18:1 (9Z) and *m*/*z* 199 and *m*/*z*

DOI: 10.1021/acs.analchem.7b04675
Anal. Chem. 2018, 90, 5612−5619

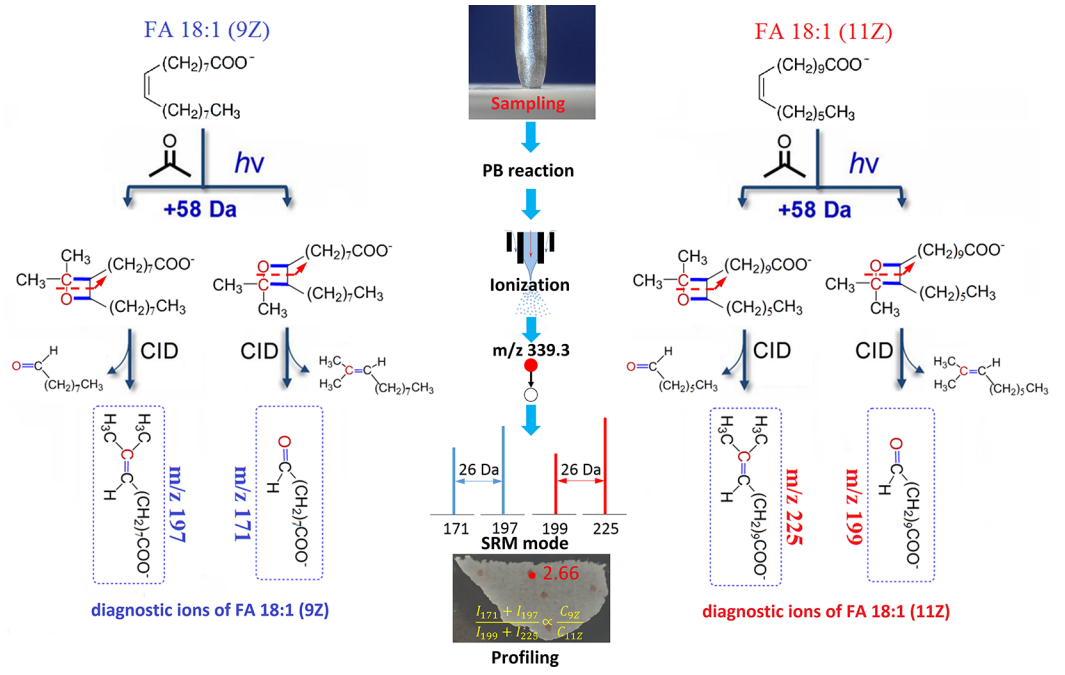

Figure 2. Analytical workflow of rapid unsaturated lipid isomer profiling and schematic representation of PB reactions and formation of C=C diagnostic ions from lipid C=C location isomers FA 18:1 (9Z) and FA 18:1 (11Z).

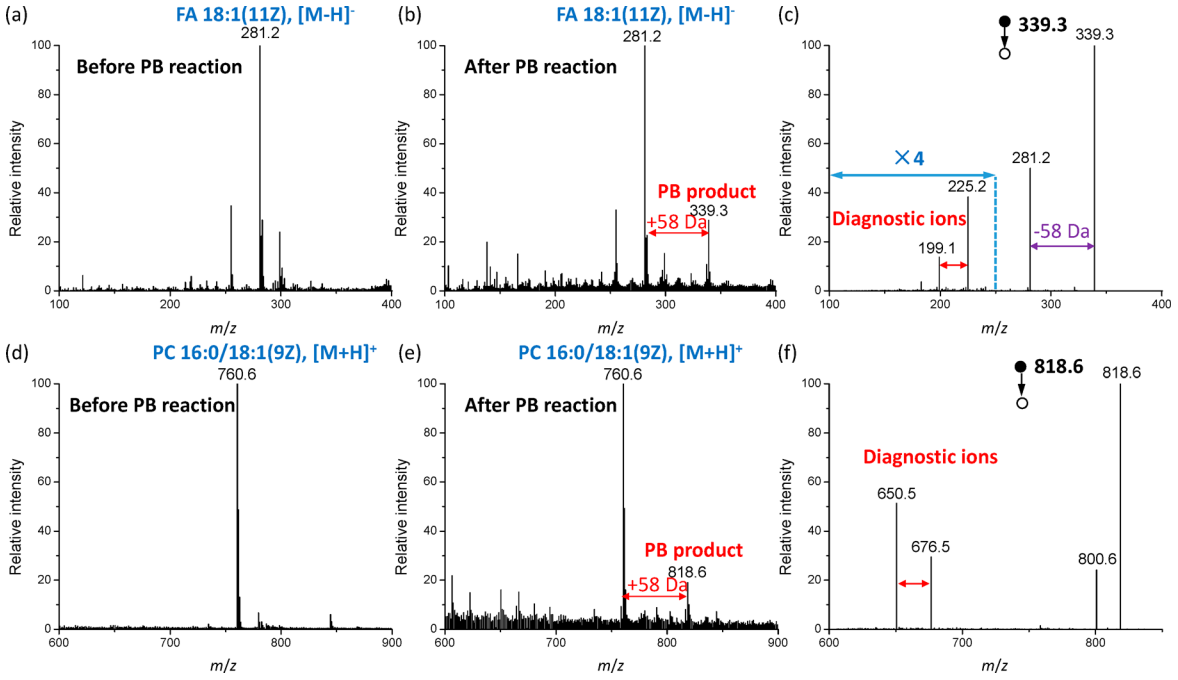

Figure 3. Mass spectra of FA 18:1 (11Z) and PC 16:0/18:1 (9Z) solution deposited on a glass slide and analyzed by LMJ-SSP/PB reaction/ESI. (a) Full scan of FA 18:1 (11Z) in negative ion mode before PB reaction. (b) Full scan of FA 18:1 (11Z) in negative ion mode after PB reaction. (c) MS/MS spectrum of m/z 339. (d) Full scan of PC 16:0/18:1 (9Z) in positive ion mode before PB reaction. (e) Full scan of PC 16:0/18:1 (9Z) in positive ion mode after PB reaction. (f) MS/MS spectrum of m/z 818.

225 for FA 18:1 (11Z). The ion abundance ratio of I_{9Z} (the sum of the ion abundance of m/z 171 and the ion abundance of m/z 197) to I_{11Z} (the sum of the ion abundance of m/z 199 and the ion abundance of m/z 225) was proportional to the concentration ratio (C_{9Z}/C_{9Z}). This relationship can be used for the relative quantitation of FA C=C location isomers.

Method Validation and Optimization of Experimental Parameters. The results of testing the apparatus using FA 18:1 (11Z) and PC 16:0/18:1 (9Z) are shown in Figure 3. Lipids were directly extracted by the extraction solvent and then analyzed. Without PB reaction, i.e., with the UV lamp turned off, there were only lipid peaks. With PB reaction, the PB products were observed. The MS^2 CID mass spectra of PB products are also shown in Figure 3c and f, where diagnostic ions are present. Similar results were obtained for the rat brain tissue section (Figure 4).

DOI: 10.1021/acs.analchem.7b04675
Anal. Chem. 2018, 90, 5612−5619

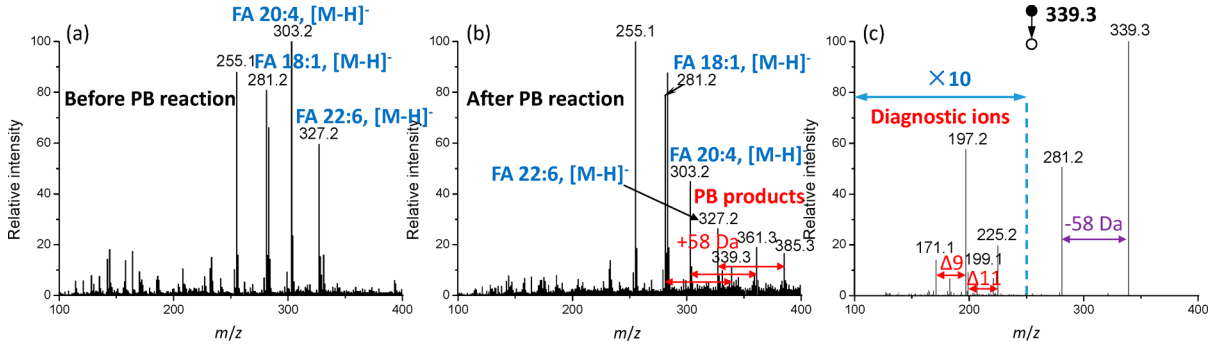

Figure 4. Mass spectrum of rat brain section by LMJ-SSP/PB reaction/ESI in negative ion mode before (a) and after (b) PB reaction. (c) MS/MS spectrum of the PB reaction products at m/z 339.3.

The reaction time, i.e., the length of UV irradiation region, was critical and was required to ensure that the reaction could be carried out adequately. Therefore, the experiment was conducted to optimize the reaction time (Figure S3). Finally, a time of 50 s was selected, corresponding to ~10 cm long UV irradiation region. In addition to the reaction time, the formulation of extraction solvent was equally important. It needed a high extraction efficiency for the lipids, a high efficiency for the PB reaction, and a high ionization efficiency for PB reaction products. Several formulations of solvents were tested (Figures S4 and S5). Solvents of 70/30 acetone/water (v/v) with 1% ammonium hydroxide as well as 60/20/20 acetone/methanol/water (v/v/v) with 1% formic acid were found to provide the optimal performance for the analyses of FA and PC, respectively.

Relative Quantitation of FA 18:1 C═C Location Isomers. Quantitation based on diagnostic ion abundances was tested with a series of mixtures of FA 18:1 9Z and 11Z isomers. Extracted ion chromatograms for FA 18:1 (9Z) and FA 18:1 (11Z) are shown in Figure 5a, which were recorded

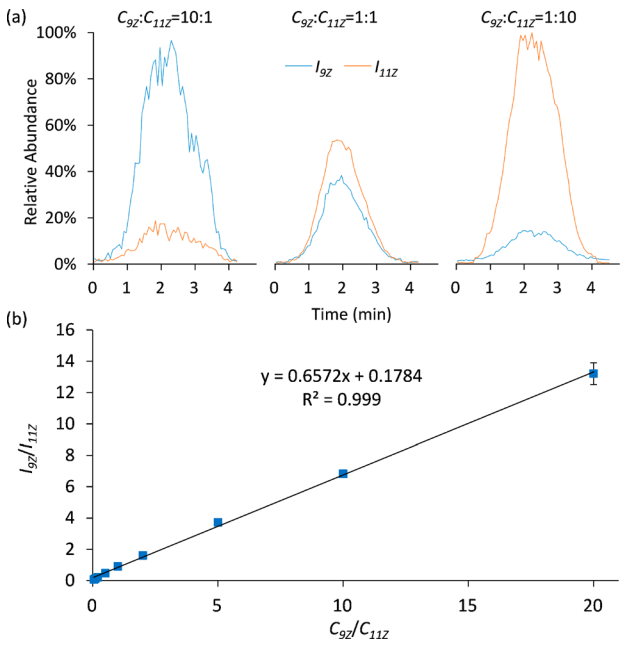

Figure 5. (a) Extracted ion chromatogram for FA 18:1 (9Z) and FA 18:1 (11Z) obtained from a standard mixture in different proportions. (b) Linear relationship established between diagnostic ion ratio and molar ratio of the two FA 18:1 C═C location isomers.

with the probe passing across a sample area on a PTFE slide at a speed of 25 μm/s. As shown in Figure 5a, the sum of I_{9Z} and I_{11Z} roughly remained unchanged because the total concentration was constant, whereas the relative abundance of I_{9Z} and I_{11Z} varies while the molar ratios (C_{9Z}/C_{11Z}) change. The ion abundance ratio (I_{9Z}/I_{11Z}) was plotted as a function of the concentration ratio (C_{9Z}/C_{11Z}), as shown in Figure 5b. A good reproducibility (RSD < 10%, 5 sampling points at each concentration ratio) and a good linearity (R^2 = 0.999) were obtained. Here, on account of lack of standards, we did not establish the linear relationship between diagnostic ion ratio and molar ratio of PC 16:0−18:1 C═C location isomers. However, the result of FA 18:1 is similar to the quantitative result obtained by nanoelectrospray ionization (NanoESI) method.[9] Using NanoESI, the linear relationship of the PC 18:1/18:1 C═C location isomers was also established.[9] These linear relationships demonstrate the effectiveness of this method for relative quantitation of lipid C═C location isomers.

Unsaturated Lipid Analysis from Rat Tissue Sections. Analysis of lipid C═C location isomers was performed for tissue sections taken from the rat brain, lung, liver, spleen, and kidney using LMJ-SSP/PB reaction/ESI apparatus, with particular focus on Δ9 and Δ11 isomers of FA 18:1 and PC16:0−18:1. Given that the background free fatty acids in solvents were likely to have impact on the results, signal-to-noise ratio (S/N) should be calculated for evaluating the effect. The average S/N of the rat tissue section data was ~25, and the maximum was up to 100. Due to the relatively low background intensity of the PC 16:0−18:1 diagnostic ions, the S/N could reach >200 (Figure S6). Therefore, the influence of background could be ignored. The ion abundance ratios of $I_{\Delta 9}/I_{\Delta 11}$ were calculated to characterize the relative quantities of Δ9 and Δ11 isomers. $I_{\Delta 9}$ was the sum of the abundance of Δ9 diagnostic ions, i.e., m/z 171 and m/z 197 for FA 18:1 or m/z 650 and m/z 676 for PC16:0−18:1; $I_{\Delta 11}$ was the sum of the abundance of Δ11 diagnostic ions, i.e., m/z 199 and m/z 225 for FA 18:1 or m/z 678 and m/z 704 for PC16:0−18:1. As shown in Figure 6, for both FA 18:1 and PC16:0−18:1, the content of Δ9 isomer was higher than the content of Δ11 isomer in all tissue sections, particularly in rat brain and lung sections. For different regions of any individual tissue section, differences in isomeric ratios for FA 18:1 and PC 16:0−18:1 were more noticeable for rat brain (standard deviation (SD) = 0.37 and 0.62) and kidney (SD = 0.24 and 0.28) than for lung (SD = 0.16 and 0.06), liver (SD = 0.11 and 0.06), and spleen (SD = 0.15 and 0.04). The Kruskall−Wallis test was used to determine whether differences in relative quantity of Δ9 and Δ11 isomers between these

DOI: 10.1021/acs.analchem.7b04675
Anal. Chem. 2018, 90, 5612−5619

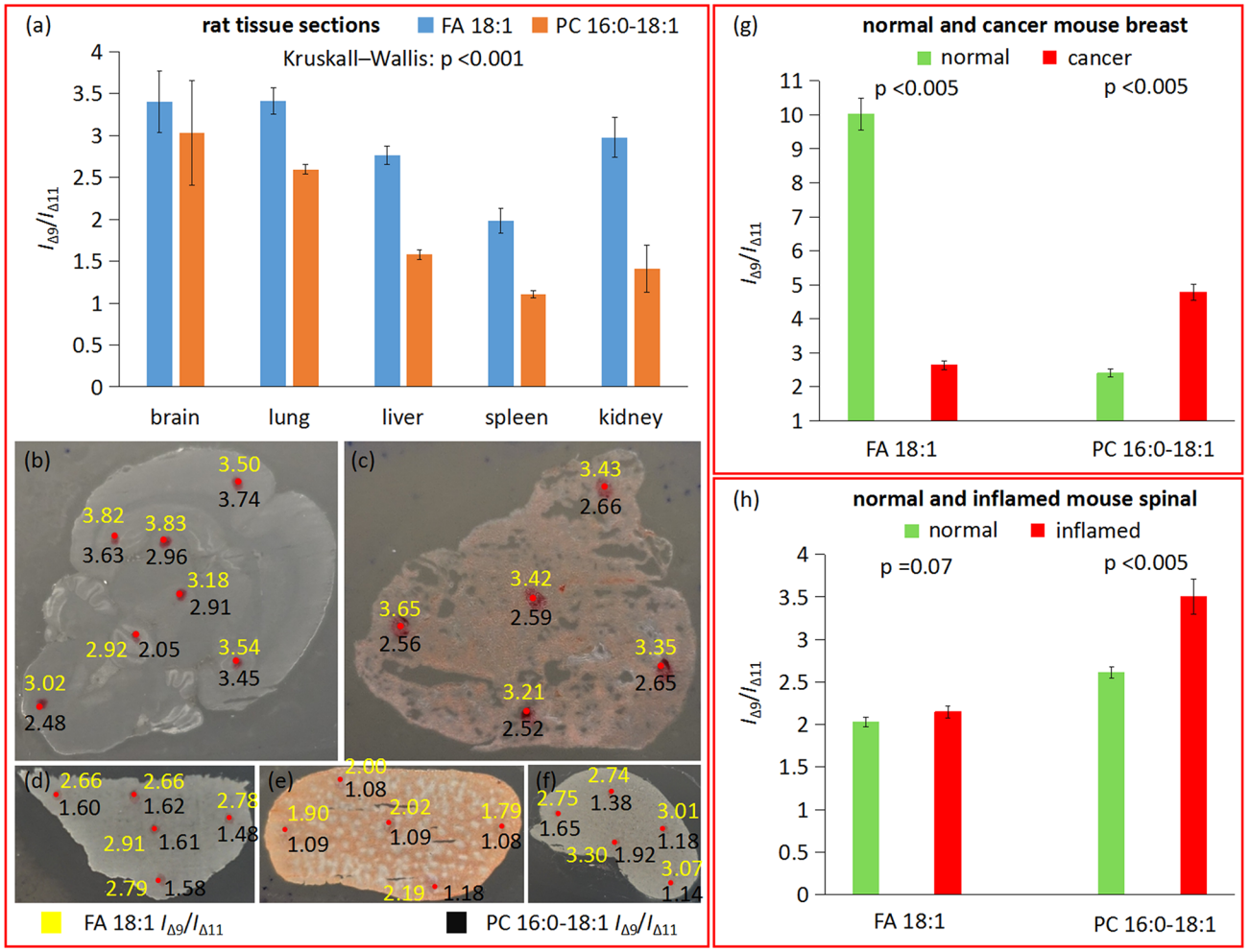

Figure 6. (a) Isomeric ratio of FA 18:1 and PC 16:0−18:1 (Δ9 to Δ11) distributed in (b) rat brain section, (c) lung section, (d) liver section, (e) spleen section, and (f) kidney section (red dots are sampling points). (g) Isomeric ratio of FA 18:1 and PC 16:0−18:1 (Δ9 to Δ11) in normal and cancerous mouse breast tissue (5 sampling points) and (h) normal and inflamed mouse spinal tissue (5 sampling points).

organs were statistically significant. p values of <0.001 for both FA 18:1 and PC 16:0−18:1 were considered statistically significant. We also analyzed some other kinds of unsaturated FAs and glycerophospholipids in rat brain section, and the results are described in the Supporting Information.

Application in the Analysis of Diseased Tissues. The lipid C═C location isomer compositions could potentially serve as biomarkers for disease diagnosis.[9] As a preliminary test for this purpose, we analyzed lipid C═C isomer compositions in normal and diseased rat breast tissues (5 sampling points), with particular focus on the Δ9 and Δ11 isomers of FA 18:1 and PC16:0−18:1. As shown in Figure 6g, the ion abundance ratios ($I_{\Delta9}/I_{\Delta11}$) show significant changes for FA 18:1 and PC16:0−18:1 between normal and cancer breast tissues. Two-sample t test statistics was used to determine whether differences between compared samples were statistically significant. Differences with p values of <0.005 were considered statistically significant. A similar result was obtained for PC16:0−18:1 between normal and inflamed mouse spinal tissues (Figure 6h), for which the p value was also <0.005. However, there was no significant change for FA 18:1 between the normal and inflamed mouse spinal cord tissues. The $I_{\Delta9}/I_{\Delta11}$ ratio was only slightly higher in the inflamed spinal cord. The t test yielded a p value of 0.07, so the difference was not statistically significant.

CONCLUSIONS

A novel method for the rapid and in situ profiling of unsaturated lipid isomers based on surface sampling and PB reaction was developed and validated for the direct analysis of FA and PC C═C location isomers in tissue. Generally, the analysis results can be achieved in <2 min without sample pretreatment. In addition to fast analysis, there are also several unique advantages, including good reproducibility (RSD < 10%), wide applicability to different lipid classes, simplicity of implementation, and compatibility with commercial MS instruments with lower-energy CID capability. More importantly, the calibration curve (R^2 = 0.999) for the relative quantitation of FA 18:1 9Z and 11Z isomers was constructed, which demonstrated the possibility for the relative quantitation of lipid C═C location isomers using this method. This method was applied for the relative quantitation of lipid C═C location isomers in tissue sections from rat brain, lung, liver, spleen, and kidney. The result indicates that there was a statistically significant difference in isomeric ratios between these organs. As a preliminary test for clinical diagnosis, lipid C═C isomer compositions in rat normal and diseased tissues were also analyzed. The results clearly show that significant differences in C═C location isomer compositions exist between normal and diseased tissues. With further developments, we believe that

DOI: 10.1021/acs.analchem.7b04675
Anal. Chem. 2018, 90, 5612−5619

LMJ-SSP/PB reaction/ESI should serve as a rapid analytical method for tissue analysis and clinical examination.

■ ASSOCIATED CONTENT

Supporting Information

The Supporting Information is available free of charge on the ACS Publications website at DOI: 10.1021/acs.analchem.7b04675.

LMJ-SSP/PB reaction/ESI apparatus; optimization of the apparatus conditions; analysis of unsaturated lipids in rat tissue sections; disease tissue analysis (PDF)

■ AUTHOR INFORMATION

Corresponding Authors

*E-mail: tangf@tsinghua.edu.cn.
*E-mail: ouyang@tsinghua.edu.cn.

ORCID

Fei Tang: 0000-0001-8155-1178
Xiaoxiao Ma: 0000-0003-1205-6485
Yu Xia: 0000-0001-8694-9900

Author Contributions

‡F.T. and C.G. contributed equally to this work and share the first authorship.

Notes

The authors declare no competing financial interest.

■ ACKNOWLEDGMENTS

This work was financially supported by the National Natural Science Foundation of China (51575312) and the Fundamental Research Project of Shenzhen (JCYJ20150601165744636).

■ REFERENCES

(1) Fahy, E.; Subramaniam, S.; Brown, H. A.; Glass, C. K.; Merrill, A. H.; Murphy, R. C.; Raetz, C. R. H.; Russell, D. W.; Seyama, Y.; Shaw, W.; Shimizu, T.; Spener, F.; van Meer, G.; VanNieuwenhze, M. S.; White, S. H.; Witztum, J. L.; Dennis, E. A. *J. Lipid Res.* **2005**, *46*, 839−862.
(2) Orešič, M.; Hänninen, V. A.; Vidal-Puig, A. *Trends Biotechnol.* **2008**, *26*, 647−652.
(3) Uauy, R.; Mena, P.; Rojas, C. *Proc. Nutr. Soc.* **2000**, *59*, 3−15.
(4) Uauy, R.; Peirano, P.; Hoffman, D.; Mena, P.; Birch, D.; Birch, E. *Lipids* **1996**, *31*, S167−S176.
(5) Calder, P. C. *Clin. Sci.* **2004**, *107*, 1−11.
(6) Martinez-Seara, H.; Róg, T.; Pasenkiewicz-Gierula, M.; Vattulainen, I.; Karttunen, M.; Reigada, R. *J. Phys. Chem. B* **2007**, *111*, 11162−11168.
(7) Martinez-Seara, H.; Róg, T.; Pasenkiewicz-Gierula, M.; Vattulainen, I.; Karttunen, M.; Reigada, R. *Biophys. J.* **2008**, *95*, 3295−3305.
(8) Yang, K.; Dilthey, B. G.; Gross, R. W. *Anal. Chem.* **2013**, *85*, 9742−9750.
(9) Ma, X.; Chong, L.; Tian, R.; Shi, R.; Hu, T. Y.; Ouyang, Z.; Xia, Y. *Proc. Natl. Acad. Sci. U. S. A.* **2016**, *113*, 2573−2578.
(10) Wilson, R.; Sargent, J. R. *J. Chromatogr. A* **1992**, *623*, 403−407.
(11) von Rudloff, E. *J. Am. Oil Chem. Soc.* **1956**, *33*, 126−128.
(12) Thies, W. *Fat Sci. Technol.* **1995**, *97*, 411−413.
(13) Christie, W. W.; Breckenridge, G. H. M. *J. Chromatogr. A* **1989**, *469*, 261−269.
(14) Sun, C.; Zhao, Y.; Curtis, J. M. *Anal. Chim. Acta* **2013**, *762*, 68−75.
(15) Kozlowski, R. L.; Campbell, J. L.; Mitchell, T. W.; Blanksby, S. J. *Anal. Bioanal. Chem.* **2015**, *407*, 5053−5064.
(16) Pham, H. T.; Ly, T.; Trevitt, A. J.; Mitchell, T. W.; Blanksby, S. J. *Anal. Chem.* **2012**, *84*, 7525−7532.
(17) Brown, S. H. J.; Mitchell, T. W.; Blanksby, S. J. *Biochim. Biophys. Acta, Mol. Cell Biol. Lipids* **2011**, *1811*, 807−817.
(18) Hsu, F.; Turk, J. *J. Am. Soc. Mass Spectrom.* **2008**, *19*, 1681−1691.
(19) Thomas, M. C.; Mitchell, T. W.; Harman, D. G.; Deeley, J. M.; Murphy, R. C.; Blanksby, S. J. *Anal. Chem.* **2007**, *79*, 5013−5022.
(20) Yoo, H. J.; Håkansson, K. *Anal. Chem.* **2010**, *82*, 6940−6946.
(21) Deimler, R. E.; Sander, M.; Jackson, G. P. *Int. J. Mass Spectrom.* **2015**, *390*, 178−186.
(22) Campbell, J. L.; Baba, T. *Anal. Chem.* **2015**, *87*, 5837−5845.
(23) Liang, X.; Liu, J.; LeBlanc, Y.; Covey, T.; Ptak, A. C.; Brenna, J. T.; McLuckey, S. A. *J. Am. Soc. Mass Spectrom.* **2007**, *18*, 1783−1788.
(24) Cohen, S. L. *Anal. Chem.* **2006**, *78*, 4352−4362.
(25) Nishikawa, K.; Hashimoto, M.; Itoh, Y.; Hiroi, S.; Kusai, A.; Hirata, F.; Sakamoto, T.; Iwaya, K. *FEBS Open Bio* **2014**, *4*, 179−184.
(26) Huang, M.; Yuan, C.; Cheng, S.; Cho, Y.; Shiea, J. *Annu. Rev. Anal. Chem.* **2010**, *3*, 43−65.
(27) Cheng, S.; Shiea, C.; Huang, Y.; Wang, C.; Cho, Y.; Shiea, J. *Anal. Methods* **2017**, *9*, 4924−4935.
(28) Jarmusch, A. K.; Pirro, V.; Baird, Z.; Hattab, E. M.; Cohen-Gadol, A. A.; Cooks, R. G. *Proc. Natl. Acad. Sci. U. S. A.* **2016**, *113*, 1486−1491.
(29) Wang, H.; Manicke, N. E.; Yang, Q.; Zheng, L.; Shi, R.; Cooks, R. G.; Ouyang, Z. *Anal. Chem.* **2011**, *83*, 1197−1201.
(30) Alfaro, C. M.; Jarmusch, A. K.; Pirro, V.; Kerian, K. S.; Masterson, T. A.; Cheng, L.; Cooks, R. G. *Anal. Bioanal. Chem.* **2016**, *408*, 5407−5414.
(31) Mandal, M. K.; Yoshimura, K.; Chen, L. C.; Yu, Z.; Nakazawa, T.; Katoh, R.; Fujii, H.; Takeda, S.; Nonami, H.; Hiraoka, K. *J. Am. Soc. Mass Spectrom.* **2012**, *23*, 2043−2047.
(32) Astigarraga, E.; Barreda-Gómez, G.; Lombardero, L.; Fresnedo, O.; Castaño, F.; Giralt, M. T.; Ochoa, B.; Rodríguez-Puertas, R.; Fernández, J. A. *Anal. Chem.* **2008**, *80*, 9105−9114.
(33) Alberici, L. C.; Oliveira, H. C. F.; Catharino, R. R.; Vercesi, A. E.; Eberlin, M. N.; Alberici, R. M. *Anal. Bioanal. Chem.* **2011**, *401*, 1651−1659.
(34) Shrestha, B.; Nemes, P.; Nazarian, J.; Hathout, Y.; Hoffman, E. P.; Vertes, A. *Analyst* **2010**, *135*, 751−758.
(35) Liu, J.; Cooks, R. G.; Ouyang, Z. *Anal. Chem.* **2011**, *83*, 9221−9225.
(36) Luo, Z.; He, J.; Chen, Y.; He, J.; Gong, T.; Tang, F.; Wang, X.; Zhang, R.; Huang, L.; Zhang, L.; Lv, H.; Ma, S.; Fu, Z.; Chen, X.; Yu, S.; Abliz, Z. *Anal. Chem.* **2013**, *85*, 2977−2982.
(37) Almeida, R.; Berzina, Z.; Arnspang, E. C.; Baumgart, J.; Vogt, J.; Nitsch, R.; Ejsing, C. S. *Anal. Chem.* **2015**, *87*, 1749−1756.
(38) Lanekoff, I.; Burnum-Johnson, K.; Thomas, M.; Cha, J.; Dey, S. K.; Yang, P.; Prieto Conaway, M. C.; Laskin, J. *Anal. Bioanal. Chem.* **2015**, *407*, 2063−2071.
(39) Ifa, D. R.; Eberlin, L. S. *Clin. Chem.* **2016**, *62*, 111−123.
(40) Ferreira, C. R.; Yannell, K. E.; Jarmusch, A. K.; Pirro, V.; Ouyang, Z.; Cooks, R. G. *Clin. Chem.* **2016**, *62*, 99.
(41) Eberlin, L. S.; Norton, I.; Dill, A. L.; Golby, A. J.; Ligon, K. L.; Santagata, S.; Cooks, R. G.; Agar, N. Y. R. *Cancer Res.* **2012**, *72*, 645−654.
(42) Calligaris, D.; Caragacianu, D.; Liu, X.; Norton, I.; Thompson, C. J.; Richardson, A. L.; Golshan, M.; Easterling, M. L.; Santagata, S.; Dillon, D. A.; Jolesz, F. A.; Agar, N. Y. R. *Proc. Natl. Acad. Sci. U. S. A.* **2014**, *111*, 15184−15189.
(43) Balog, J.; Sasi-Szabó, L.; Kinross, J.; Lewis, M. R.; Muirhead, L. J.; Veselkov, K.; Mirnezami, R.; Dezső, B.; Damjanovich, L.; Darzi, A.; Nicholson, J. K.; Takáts, Z. *Sci. Transl. Med.* **2013**, *5*, 194ra93.
(44) Balog, J.; Szaniszlo, T.; Schaefer, K.; Denes, J.; Lopata, A.; Godorhazy, L.; Szalay, D.; Balogh, L.; Sasi-Szabo, L.; Toth, M.; Takats, Z. *Anal. Chem.* **2010**, *82*, 7343−7350.
(45) Zhang, J.; Rector, J.; Lin, J. Q.; Young, J. H.; Sans, M.; Katta, N.; Giese, N.; Yu, W.; Nagi, C.; Suliburk, J.; Liu, J.; Bensussan, A.; DeHoog, R. J.; Garza, K. Y.; Ludolph, B.; Sorace, A. G.; Syed, A.; Zahedivash, A.; Milner, T. E.; Eberlin, L. S. *Sci. Transl. Med.* **2017**, *9*, eaan3968.

DOI: 10.1021/acs.analchem.7b04675
Anal. Chem. 2018, 90, 5612−5619

(46) Chen, L. C.; Naito, T.; Tsutsui, S.; Yamada, Y.; Ninomiya, S.; Yoshimura, K.; Takeda, S.; Hiraoka, K. *Analyst* **2017**, *142*, 2735−2740.
(47) Shi, R.; El Gierari, E. T. M.; Faix, J. D.; Manicke, N. E. *Clin. Chem.* **2016**, *62*, 295−299.
(48) Manicke, N. E.; Bills, B. J.; Zhang, C. *Bioanalysis* **2016**, *8*, 589−606.
(49) Zhang, J. I.; Tao, W. A.; Cooks, R. G. *Anal. Chem.* **2011**, *83*, 4738−4744.
(50) Kozlowski, R. L.; Mitchell, T. W.; Blanksby, S. J. *Sci. Rep.* **2015**, *5*, 9243.
(51) Ellis, S. R.; Hughes, J. R.; Mitchell, T. W.; Panhuis, M. I. H.; Blanksby, S. J. *Analyst* **2012**, *137*, 1100−1110.
(52) Ma, X.; Xia, Y. *Angew. Chem.* **2014**, *126*, 2630−2634.
(53) Van Berkel, G. J.; Sanchez, A. D.; Quirke, J. M. E. *Anal. Chem.* **2002**, *74*, 6216−6223.
(54) Kertesz, V.; Ford, M. J.; Van Berkel, G. J. *Anal. Chem.* **2005**, *77*, 7183−7189.
(55) ElNaggar, M. S.; Van Berkel, G. J. *J. Am. Soc. Mass Spectrom.* **2011**, *22*, 1737−1743.
(56) Griffiths, R. L.; Randall, E. C.; Race, A. M.; Bunch, J.; Cooper, H. J. *Anal. Chem.* **2017**, *89*, 5683−5687.
(57) Kertesz, V.; Van Berkel, G. J. *Bioanalysis* **2013**, *5*, 819−826.
(58) Kertesz, V.; Weiskittel, T. M.; Van Berkel, G. J. *Anal. Bioanal. Chem.* **2015**, *407*, 2117−2125.

DOI: 10.1021/acs.analchem.7b04675
Anal. Chem. 2018, 90, 5612−5619